DALTON

# Synthesis, molecular structure and palladium(II) and platinum(II) complex chemistry of 3-(ferrocen-1-yl)-1-(pyridin-2-yl)pyrazole†

**Robert J. Less, Joseph L. M. Wicks, Nicholas P. Chatterton, Michael J. Dewey, Natalie L. Cromhout, Malcolm A. Halcrow* and John E. Davies**

*Department of Chemistry, University of Cambridge, Lensfield Road, Cambridge CB2 1EW, UK*

Treatment of the potassium salt of 3(5)-(ferrocen-1-yl)pyrazole $L^1$ with 2-bromopyridine in diglyme (2,5,8-trioxononane) at 130 °C for 3 d, followed by an aqueous quench, yielded the compound 3-(ferrocen-1-yl)-1-(pyridin-2-yl)pyrazole $L^2$ in 37% recrystallised yield. A single-crystal structure determination of $L^2$ confirmed the proposed 1,3-disubstitution pattern at the pyrazole ring, the substituted cyclopentadienyl and two heterocyclic rings being approximately coplanar. Treatment of $L^2$ with a stoichiometric amount of $[\{MCl(C_3H_5)\}_x]$ (M = Pd, $x$ = 2; M = Pt, $x$ = 4) and $NH_4PF_6$ gave $[M(\eta^3\text{-}C_3H_5)(L^2)]PF_6$ (M = Pd **1** or Pt **2**) while a similar reaction with $[PdCl_2(NCPh)_2]$ afforded $[PdCl_2(L^2)]$ **3**. Treatment of **3** with 1 molar equivalent of $K_2C_2O_4$, $Na_2(cat)$ or Na(acac)–$NH_4PF_6$ yielded $[Pd(L)L^2]$ [L = $C_2O_4^{2-}$ **4** or catecholate (cat) **5**] and $[Pd(acac)(L^2)]PF_6$ **6** (acac = acetylacetonate) as analytically pure solids. The $^1H$ NMR behaviour of **4**–**6** is complex and suggestive of extensive ligand dissociation in solution; molecular models imply that this may reflect steric interactions between the pendant ferrocenyl moiety and metal-bound anionic chelate O-donors. The UV/VIS and electrochemical data show that the ferrocenyl group becomes significantly electron-poorer upon co-ordination of $L^2$, reflecting an inductive interaction with the co-ordinated $M^{2+}$ (M = Pd or Pt) electrophiles.

The synthesis of 3(5)-(ferrocen-1-yl)pyrazole $L^1$ was first reported in the early 1960s.[1] However, despite the continuing interest in ferrocene-containing molecules (which have applications in non-linear optics,[2] electrochemical devices[3] and catalysis[4]), and the versatility of pyrazoles as building blocks in polydentate ligands for metal ions,[5,6] only two examples of compounds based on $L^1$ or its derivatives have thus far appeared.[7,8] By contrast, ferrocene-substituted polypyridyls have been extensively studied as ligands for transition metals.[9–11] As part of our studies of transition-metal complexes bearing redox-active pendants,[12] we report here the synthesis of the bidentate compound 3-(ferrocen-1-yl)-1-(pyridin-2-yl)pyrazole $L^2$, and a study of its palladium(II) and platinum(II) complex chemistry. We were particularly interested in $L^2$ since this is essentially a regioisomer of the recently reported 5-(ferrocen-1-yl)-3-methyl-1-(pyridin-2-yl)pyrazole $L^3$,[8] and we wished to compare the redox, spectroscopic and ligating properties of these two molecules.

## Results and Discussion

### Ligand synthesis and structure

Deprotonation of 3(5)-ferrocenylpyrazole $L^1$ with KH in diglyme (2,5,8-trioxanonane) under $N_2$ affords the potassium pyrazolide salt *in situ*, which was treated with 2-bromopyridine at 130 °C for 3 d to afford a dark brown solid after an aqueous quench. Extraction of the crude solid with hot hexanes gave the orange solid product $L^2$ in 37% overall yield (Scheme 1). While preparations of this type generally give yields approaching 70%,[13] we ascribe the low yield of $L^2$ to the previously noted[7] thermal sensitivity of $L^1$, which decomposes thermally at 150 °C in the solid. We cleanly isolated a single isomer of $L^2$ from this synthesis according to NMR spectroscopy [Fig. 1(*a*)], despite the possibility of 1,3 and 1,5 regioisomerism in the product (Scheme 1); preparations of 1-(pyridin-2-yl)pyrazoles by this method are generally completely selective for the less-hindered 1,3-disubstituted form.[13]

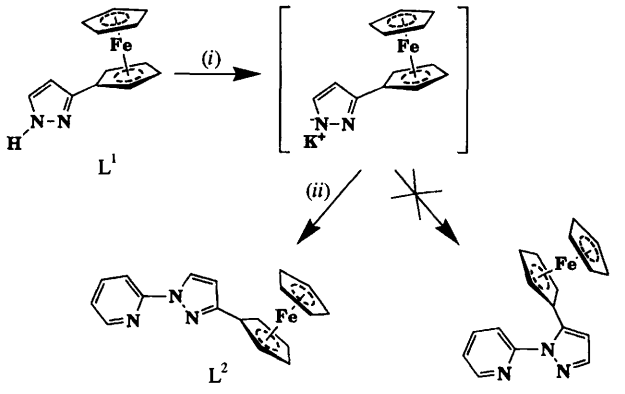

**Scheme 1** (*i*) KH, diglyme, room temperature, $N_2$, 1 h; (*ii*) 2-bromopyridine, diglyme, 130 °C, 3 d; water quench; recrystallisation from hexanes

Our attempts unambiguously to assign the regiochemistry of $L^2$ by two commonly employed NMR criteria were unsuccessful. First, it has been shown that the $H^5$ resonance in 1,3-disubstituted pyrazoles is solvent dependent, moving to higher frequency in the sequence $C_6D_6$ > $CDCl_3$ > $(CD_3)_2SO$; $H^3$ of 1,5-disubstituted pyrazoles shifts to lower frequencies between these solvents.[14] While the chemical shift of $H^{3/5}$ in $L^2$ does vary between solvents, neither of the above trends is observed [in $C_6D_6$, $\delta(H^{3/5})$ 8.71; in $CDCl_3$, 8.51; in $(CD_3)_2SO$, 8.57]. Secondly, the magnitude of $^2J(C^{3/5}\text{–}H^4)$ has employed as a fingerprint, 1,3-disubstituted pyrazoles having been proposed to exhibit $^2J(C^{3/5}\text{–}H)$ = 8–10 Hz and 1,5-disubstituted isomers $^2J(C^{3/5}\text{–}H)$ = 4–6 Hz.[15] For $L^2$ however, $^2J(C^{3/5}\text{–}H)$ = 6.5 Hz in $CDCl_3$ solution. In order

---

† Abbreviations used: Hacac = acetylacetone; $H_2cat$ = catechol; dppe = 1,2-bis(diphenylphosphino)ethane; fbipy = 6-(ferrocen-1-yl)-2,2′-bipyridyl; fpy = 2-(ferrocen-1-yl)pyridine; fterpy = 4′-(ferrocen-1-yl)-2,2′:6′,2″-terpyridine; pypz = 1-(pyridin-2-yl)pyrazole; dmppz, 3,5-dimethyl-1-(pyridin-2-yl)pyrazole. cod = cycloocta-1,5-diene; nbd = bicyclo[2.2.1]hepta-2,5-diene (norbornadiene).

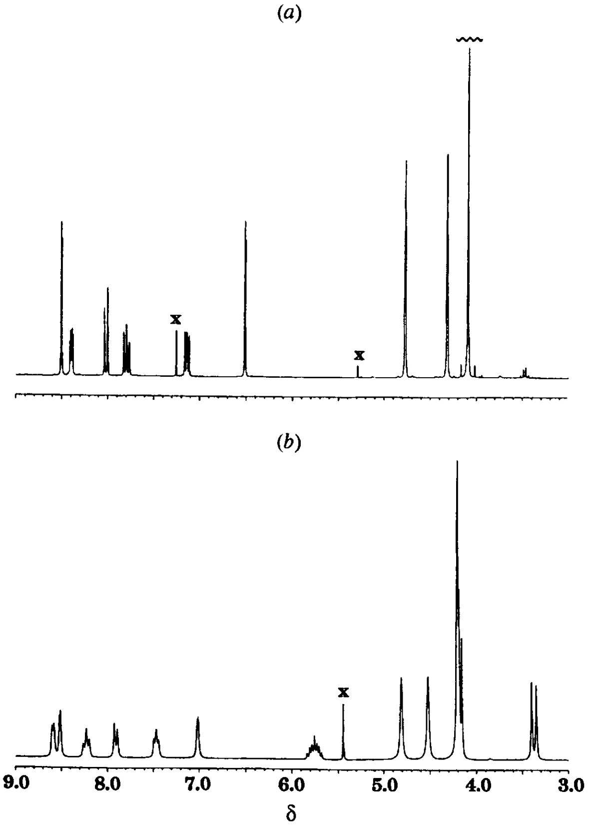

**Fig. 1** Proton NMR spectra (250 MHz, 293 K) of (*a*) $L^2$ ($CDCl_3$) and (*b*) $[Pd(\eta^3-C_3H_5)(L^2)]PF_6$ ($CD_3CN$). Peaks marked × at δ 7.2 and 5.5 are due to $CHCl_3$ and $CH_2Cl_2$ respectively

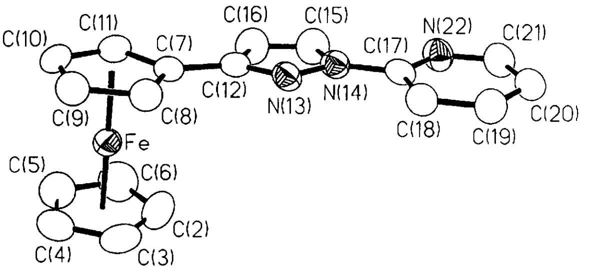

**Fig. 2** Solid-state structure of $L^2$, showing the atom numbering scheme employed. Thermal ellipsoids are at the 50% probability level. For clarity, all hydrogen atoms have been omitted

unambiguously to assign the molecular structure of this compound, therefore, a single-crystal X-ray analysis was undertaken.

The molecular structure of $L^2$ is shown in Fig. 2, bond lengths and angles in Table 1. The unit cell contains one molecule of $L^2$, which exhibits the expected 1,3-disubstitution pattern, lying on a general position. The substituted and non-substituted cyclopentadienyl rings are symmetrically disposed about the iron atom, with Fe(1)–X(1) 1.649, Fe(1)–X(2) 1.642 Å and X(1)–Fe–X(2) 179.6° [X(1) and X(2) are the centroids of the C(2)–C(6) and C(7)–C(11) cyclopentadienyl rings, respectively]. The structural indices for the pyrazole ring, $\Delta N = 6.4°$ and $10^2\Delta r_{CN} = 3.7$ Å $\{\Delta N = [N(13)–N(14)–C(15)] - [C(12)–N(13)–N(14)]$; $\Delta r_{CN} = [N(14)–C(15)] - [C(12)–N(13)]\}$, are within the usual ranges for 1-arylpyrazoles.[16] The substituted $C_5H_4$ and two heterocyclic groups are almost coplanar, with cyclopentadienyl–pyrazole and pyrazole–pyridinyl dihedral angles of 8.6(2) and 5.7(2)° respectively. The molecules pack in the crystal *via* an intermolecular graphitic interaction between the $C_5H_5^-$ ring on one molecule and a neighbouring pyridinyl group, the closest interatomic distance and dihedral angle between the two residues being 3.500(5) Å and 8.1(2)°.

## Syntheses and NMR spectra of complexes

Reaction of $[\{MCl(C_3H_5)\}_x]$ (M = Pd, $x$ = 2; M = Pt, $x$ = 4) with $L^2$ and $NH_4PF_6$ in $CH_2Cl_2$ affords, after filtration and concentration of the solution, orange (M = Pd) or red (M = Pt) microcrystalline solids, whose IR, FAB mass spectra and elemental microanalyses are consistent with the formulations $[M(C_3H_5)(L^2)]PF_6$ (M = Pd **1** or Pt **2**). Once isolated, **1** and **2** are insoluble in chlorinated solvents or arenes, but moderately soluble in MeCN, $MeNO_2$ and acetone.

The 250 MHz $^1H$ NMR spectrum of complex **1** in $CD_3CN$ at 293 K, as well as showing peaks expected for co-ordinated $L^2$, is typical of a fluxional $\eta^3-C_3H_5^-$ species, exhibiting two peaks corresponding to *syn*- and *anti*-allyl $CH_2$ protons and a pseudo-septet for the central CH group [Fig. 1(*b*)]. In addition, the ferrocenyl group shows mirror symmetry, with only one resonance each for the substituted cyclopentadienyl α- and β-CH groups, both integrating to 2 H. Cooling a sample of **1** in $(CD_3)_2CO$ to −60 °C results in the onset of decoalescence of the *syn*- and *anti*-allyl $CH_2$ resonances into separate peaks corresponding to $CH_2$ groups *trans* to pyridyl and pyrazolyl N-donors; similar $T_c$ values have been reported for other fluxional palladium(II) $\eta^3$-allyls bearing asymmetric chelate ligands.[17] However, $T_c$ could not be measured accurately for **1** because these peaks, which occur at δ 4.15 and 3.42 in this solvent, were partially obscured by the $C_5H_5^-$ (δ 4.11) and water resonances respectively. By contrast, the $^1H$ NMR spectrum of **2** is static at 293 K, with separate resonances being observed for all five allyl protons, and for all four protons of the substituted $C_5H_4$ ring; similarly, six peaks were observed in the cyclopentadienyl region of the $^{13}C$ spectrum in an approximate 1 : 1 : 1 : 1 : 1 : 5 integral ratio. This can be rationalised if the pendant ferrocenyl group lies perpendicular to the ligand square plane in **1** and **2**, which for a non-fluxional molecule would render the α, α′ and β, β′ substituted cyclopentadienyl sites non-equivalent (Scheme 2).

Reaction of $[PdCl_2(NCPh)_2]$ with $L^2$ in $CH_2Cl_2$ results in the overnight precipitation in good yield of deep red sparingly soluble crystals analysing as $[PdCl_2(L^2)]$ **3**. The IR spectrum of **3** shows peaks arising from co-ordinated $L^2$ only, while its FAB mass spectrum exhibits peaks with $m/z$ = 505, 470 and 435 assignable to $[^{106}Pd^{35}Cl_x(L^2)]^+$ ($x$ = 2, 1 or 0); no higher-mass peaks were evident. We therefore formulate **3** as a mononuclear neutral square-planar complex with *cis*-chloride ligands. Proton NMR spectra of **3** in $CDCl_3$ and $CD_3CN$ both demonstrate the presence of a single species in these solvents, presumably intact **3**. However, in $(CD_3)_2SO$ three distinct species were observed; unco-ordinated $L^2$, and major and minor components assignable as $[PdCl_n\{(CD_3)_2SO\}_{2-n}L^2]^{(2-n)+}$ ($n$ = two from 2, 1 or 0). A $^{13}C$ NMR study of **3** was not attempted because of the low solubility of this complex. No reaction was observed between $[PtCl_2(NCPh)_2]$ and $L^2$ in $CH_2Cl_2$ or MeCN at room temperature, while refluxing these reactants in $CH_2Cl_2$, $CHCl_3$ or MeCN resulted in ligand decomposition.

Attempts to prepare complexes of $L^2$ orthometallated at the ferrocenyl group, following methods previously employed for the palladation of fpy and fbipy,[9c,18] were unsuccessful. Thus, treatment of **3** with $NaO_2CMe$ in MeOH at room temperature gave no reaction, while reaction under reflux resulted in ligand decomposition.[18] Similarly, reaction of $[PdCl_2(cod)]$ with $L^2$ in $CH_2Cl_2$ at room temperature[9c] afforded no isolable solid products. This may reflect the greater distance of the substituted cyclopentadienyl α-CH groups from the palladium centre in co-ordinated $L^2$ compared to metal-bound fbipy, caused by the correspondingly more obtuse N(donor)–C(bridgehead)–C(*ipso*-ferrocenyl) angles for a five-membered pyrazole rather than a six-membered pyridine ring [C(7)–C(12)–N(13) 122.2(2)° for $L^2$, while for fbipy the equivalent angle is *ca.* 112°].[9c,g]

Treatment of complex **3** with 1 molar equivalent of $K_2C_2O_4$

**Table 1** Selected bond lengths (Å) and angles (°) for compound $L^2$

| | | | |
|---|---|---|---|
| Fe–C(2) | 2.031(3) | C(7)–C(12) | 1.465(4) |
| Fe–C(3) | 2.034(4) | C(8)–C(9) | 1.431(4) |
| Fe–C(4) | 2.049(3) | C(9)–C(10) | 1.411(5) |
| Fe–C(5) | 2.043(3) | C(10)–C(11) | 1.406(5) |
| Fe–C(6) | 2.026(4) | C(12)–N(13) | 1.319(3) |
| Fe–C(7) | 2.035(3) | C(12)–C(16) | 1.414(4) |
| Fe–C(8) | 2.051(3) | N(13)–N(14) | 1.367(3) |
| Fe–C(9) | 2.046(3) | N(14)–C(15) | 1.356(4) |
| Fe–C(10) | 2.042(3) | N(14)–C(17) | 1.411(3) |
| Fe–C(11) | 2.013(3) | C(15)–C(16) | 1.360(5) |
| C(2)–C(3) | 1.402(6) | C(17)–C(18) | 1.385(4) |
| C(2)–C(6) | 1.415(6) | C(17)–N(22) | 1.331(3) |
| C(3)–C(4) | 1.396(5) | C(18)–C(19) | 1.383(4) |
| C(4)–C(5) | 1.409(6) | C(19)–C(20) | 1.375(4) |
| C(5)–C(6) | 1.406(6) | C(20)–C(21) | 1.374(4) |
| C(7)–C(8) | 1.425(4) | C(21)–N(22) | 1.334(4) |
| C(7)–C(11) | 1.416(4) | | |
| | | | |
| C(3)–C(2)–C(6) | 107.3(3) | C(12)–N(13)–N(14) | 105.1(2) |
| C(2)–C(3)–C(4) | 109.5(4) | N(13)–N(14)–C(15) | 111.5(2) |
| C(3)–C(4)–C(5) | 107.0(4) | N(13)–N(14)–C(17) | 121.2(2) |
| C(4)–C(5)–C(6) | 108.7(4) | C(15)–N(14)–C(17) | 127.3(2) |
| C(2)–C(6)–C(5) | 107.5(4) | N(14)–C(15)–C(16) | 106.9(3) |
| C(8)–C(7)–C(11) | 107.2(3) | C(12)–C(16)–C(15) | 105.4(3) |
| C(8)–C(7)–C(12) | 126.8(2) | N(14)–C(17)–C(18) | 120.8(2) |
| C(11)–C(7)–C(12) | 126.0(3) | N(14)–C(17)–N(22) | 114.9(2) |
| C(7)–C(8)–C(9) | 107.4(3) | C(18)–C(17)–N(22) | 124.3(3) |
| C(8)–C(9)–C(10) | 108.5(3) | C(17)–C(18)–C(19) | 117.4(3) |
| C(9)–C(10)–C(11) | 107.4(3) | C(18)–C(19)–C(20) | 119.5(3) |
| C(7)–C(11)–C(10) | 109.5(3) | C(19)–C(20)–C(21) | 118.0(3) |
| C(7)–C(12)–N(13) | 122.2(2) | C(20)–C(21)–N(22) | 124.5(3) |
| C(7)–C(12)–C(16) | 126.6(3) | C(17)–N(22)–C(21) | 116.2(2) |
| N(13)–C(12)–C(16) | 111.1(3) | | |

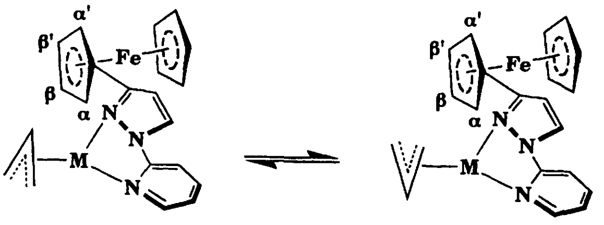

Scheme 2 Equilibration of the substituted cyclopentadienyl protons in complexes 1 and 2 *via* $\eta^3$-allyl fluxionality

or $Na_2(cat)$ in methanol yielded orange precipitates analysing as $[Pd(C_2O_4)(L^2)]$ **4** and $[Pd(cat)(L^2)]$ **5**; while **5** is sparingly soluble in MeCN and chlorinated solvents, **4** is insoluble in all common solvents except $Me_2SO$. Similarly, reaction of **3** with Na(acac) in the presence of $TlPF_6$ gave a deep red solution, from which a soluble red product $[Pd(acac)(L^2)]PF_6$ **6** was obtained by layering with $Et_2O$. Infrared spectroscopy of all these products demonstrated the presence of $L^2$, $PF_6^-$ (for **6**) and the relevant anionic chelate[19] [for **4**, $\nu_{asym}$(O–C–O) 1698, 1665; for **5**, ν(C–O) 1261; for **6**, ν(C–O) 1563, 1523 $cm^{-1}$], while the highest molecular ion by FAB mass spectrometry in each case corresponded to $[^{106}Pd(L)L^2]^+$ ($L = C_2O_4^{2-}$, *m/z* 523; $cat^{2-}$, 543; $acac^-$, 534). We therefore assign **4–6** as the expected square-planar *cis*-$[PdN_2O_2]$ chelate complexes. Attempts to prepare the dinuclear species $[(PdL^2)_2(\mu\text{-}C_2O_4)][PF_6]_2$ by treating **3** with 0.5 equivalent of $K_2C_2O_4$ in the presence of $NH_4PF_6$ afforded only reduced yields of **4**.

The $^1H$ NMR spectra of complexes **5** and **6** in $CD_3CN$ and $CDCl_3$ are complicated, demonstrating the presence of at least four distinct ferrocenyl species, none of which corresponds to unco-ordinated $L^2$. In the more co-ordinating $(CD_3)_2SO$, however, for **4–6** only two species are observed, in approximately equal populations; unco-ordinated $L^2$ and one other species which is different for each product and which we therefore ascribe to intact $[Pd(L)L^2]^{n+}$ ($L = C_2O_4^{2-}$ or $cat^{2-}$, $n = 0$; $L = acac^-$, $n = 1$). Together with the aforementioned data for **3**, this suggests that $Pd^{II}$-bound $L^2$ is relatively labile, and is partially displaced by co-ordinating solvents or other pro-ligands in solution. A similar observation regarding the solution lability of $Pd^{II}$–pypz complexes has recently been made.[17b]

Attempts to prepare other mixed-ligand palladium(II) complexes of $L^2$ by substitution of the chloride ligands in **3** were unsuccessful. Reactions of **3** with cod, nbd and dppe in the presence of an excess of $TlPF_6$ in MeCN or $MeNO_2$ afforded uniformly a maroon solid, which was also obtained from reactions of $[PdCl_2(cod)]$ or $[PdCl_2(dppe)]$ with $L^2$ and $TlPF_6$, and from treatments of **3** with 1 or 2 molar equivalents of $TlPF_6$ only, in the same solvents. Thin-layer chromatography (TLC) with MeCN-water-saturated aqueous $KNO_3$ (10:1:1) as eluent, $^1H$ NMR ($CD_3CN$) and cyclic voltammetry (MeCN–0.1 mol $dm^{-3}$ $NBu^n_4PF_6$) in each case showed the presence of two major $L^2$-containing complexes in these samples, which we were unable to separate by crystallisation. The products exhibit IR peaks arising from co-ordinated $L^2$ and $PF_6^-$ only, and a highest FAB mass peak at $m/z = 434$, corresponding to $[^{106}PdL^2 - H]^+$. In the absence of any structural data, we tentatively assign the maroon solids as mixtures of solvated complexes $[PdCl_x(solv)_{2-x}L^2][PF_6]_{2-x}$ (solv = MeCN, $MeNO_2$, $H_2O$, *etc.*; $x = 1$ or 2).

Examination of molecular models of complexes **4–6** based on the X-ray analysis of $L^2$ (see above) suggests that such structures would give rise to significant steric and/or electrostatic interactions between the negatively charged Pd-bound O-donor *trans* to the pyridyl group of $L^2$ and the substituted cyclopentadienyl π cloud, since the distance between this O atom and the bridgehead ferrocene carbon atom [C(7) of the structure analysis, Fig. 2)] is *ca.* 2.6 Å. In addition, the ferrocenyl moiety would be strongly constrained to be perpendicular to the ligand-donor square plane (Scheme 2), as rotation of this group about the C(7)–C(12) bond would bring the α-carbon atoms [C(8) and C(11)] into very close contact with the same O-donor (these atoms would lie *ca.* 1.6 Å apart when the substituted cyclopentadienyl ring is coplanar with the co-ordinated pyrazole group). For **6** there is also the possibility of steric repulsions between adjacent substituted cyclopentadienyl β-CH and $acac^-$ methyl groups, as these C atoms lie < 3 Å apart. Such steric interactions could explain our difficulties in preparing other mixed-ligand $[Pd(L)_2L^2]^{2+}$ complexes, and the complex NMR behaviour of **4–6**. The Pd ··· Fe distance in these complexes is approximately 5.5 Å.

## Electrochemistry and electronic spectroscopy

Solution UV/VIS data for $L^1$,$L^2$ and complexes **1–3** are listed in Table 2; spectra of **4–6** were not recorded because of the uncertain nature of the species present in solution. The spectrum of $L^1$ exhibits the two spin-allowed d–d absorptions expected of a ferrocene centre,[20] together with a higher-energy absorption attributable to a metal-to-ligand charge-transfer (m.l.c.t.) band of uncertain composition; the shoulder at 219 nm may correspond to a pyrazole $\pi \longrightarrow \pi^*$ transition, which generally lie between $\lambda_{max} = 210$ and 255 nm in the absence of strongly electron-withdrawing substituents.[21] N-Pyridination of the pyrazole ring in $L^2$ has no significant effect on the energies of the ferrocene d–d transitions (in the same way, the d–d maxima of 1-phenylferrocenes are only perturbed by very electron-withdrawing phenyl substituents[20a,22]), but increases their intensities. The assignment of the higher-energy absorptions for $L^2$ is complicated by additional bands arising from the pyridinylpyrazole moiety (pypz shows $\lambda_{max} = 250$ and 280 nm[23]), although interestingly the UV region for $L^2$ shows an extra absorption ($\lambda_{max} = 292$ nm) compared to that reported for $L^3$ in the same solvent.[8]

The spectra of complexes **1–3** (Table 2) demonstrate that the ferrocenyl group in $L^2$ is electronically perturbed by metal

**Table 2** The UV/VIS spectroscopic data for the compounds studied (MeCN, 293 K)

| Compound | $\lambda_{max}$/nm ($\varepsilon_{max}$/dm$^3$ mol$^{-1}$ cm$^{-1}$) |
|---|---|
| L$^1$ | 219 (sh), 273 (9100), 326 (sh), 443 (230) |
| L$^2$ | 212 (sh), 271 (sh), 292 (17 600), 322 (sh), 444 (400) |
| **1** | 268 (sh), 274 (30 200), 300 (sh), 382 (2400), 443 (sh) |
| **2** | 262 (17 300), 307 (18 700), 396 (2500), 467 (1900) |
| **3** | 205 (53 000), 213 (sh), 259 (17 300), 318 (14 100), 386 (3600), 476 (1900) |

**Table 3** Voltammetric data for the compounds studied (MeCN–0.1 mol dm$^{-3}$ NBu$^n{}_4$PF$_6$ or CH$_2$Cl$_2$–0.5 mol dm$^{-3}$ NBu$^n{}_4$PF$_6$, 293 K, 100 mV s$^{-1}$). All potentials quoted *vs.* an internal ferrocene–ferrocenium standard

| Compound | Solvent | $E_{\frac{1}{2}}$(Fe$^{II}$–Fe$^{III}$)/V | $\Delta E_p$/mV | Other peaks, $E_{Pc}$/V |
|---|---|---|---|---|
| L$^1$ | MeCN | +0.10 | 103 | — |
| | CH$_2$Cl$_2$ | +0.00 | 85 | — |
| L$^2$ | MeCN | +0.07 | 93 | — |
| | CH$_2$Cl$_2$ | +0.03 | 89 | — |
| **1** | MeCN | +0.12 | 127 | −1.66 |
| **2** | MeCN | +0.24 | 104 | −1.89 |
| **3** | MeCN | +0.12 | 98 | −2.06 |
| | CH$_2$Cl$_2$ | +0.15 | 88 | −1.98 |
| **5** | MeCN | +0.03 | 95 | +0.28,* −1.89 |
| | CH$_2$Cl$_2$ | −0.02 | 73 | +0.20,* −1.94 |
| **6** | MeCN | +0.18 | 102 | −1.31, −1.95 |
| | CH$_2$Cl$_2$ | +0.22 | 72 | −1.28 |

* Quasi-reversible $E_{\frac{1}{2}}$.

co-ordination. For each complex the two lowest-energy absorptions can be safely assigned to ferrocenyl d–d transitions, which are *ca.* 5 times as intense as for free L$^2$, although for **1–3** the lower-wavelength peak probably overlies a weaker palladium(II) d–d band;[24] [PdCl$_2$(dmppz)] exhibits such a transition at $\lambda_{max}$ = 380 nm ($\varepsilon_{max}$ = 211 dm$^3$ mol$^{-1}$ cm$^{-1}$).[25] Interestingly, the lowest ferrocenyl d–d absorption for **1** is essentially unchanged compared to uncomplexed L$^2$; however, for **2** both d–d maxima are substantially red-shifted compared to **1**. This is consistent with the greater degree of L$^2$→M σ donation expected for M = Pt compared to M = Pd, since these d–d absorptions generally move to lower energy as the substituents on the ferrocene moiety become more electron withdrawing.[20b]

The lowest-energy ferrocenyl d–d transition is substantially red-shifted for complex **3** compared to **1**, which presumably reflects the weaker donor ability of the *trans*-Cl$^-$ ligands compared to C$_3$H$_5{}^-$. The shoulder at 213 nm in the spectrum of **3** may correspond to a Cl$^-$→Pd ligand-to-metal charge-transfer (l.m.c.t.) band[24] while, given its very high intensity, the peak at $\lambda_{max}$ = 205 nm probably arises from a ferrocenyl C$_5$H$_5$→Fe l.m.c.t. transition.[20a]

The Fe$^{II}$–Fe$^{III}$ oxidation potentials for L$^1$,L$^2$ and the complexes in this study are listed in Table 3; no such measurement was possible for **4** because of its insolubility in electrochemically useful solvents. For all compounds except **5** (where this process is partially obscured by an additional ligand oxidation, see below) a plot of $I_{pa}$ *vs.* $\nu^{\frac{1}{2}}$ ($\nu$ = scan rate) for the Fe$^{II}$–Fe$^{III}$ couples gave a straight line in the range 10 < $\nu$ < 1000 mV s$^{-1}$, confirming their reversibility under these conditions. For **3**, **5** and **6**, although the voltammograms recorded showed a single detectable ferrocenyl environment, given the aforementioned NMR data the identity of the species present at the electrode is unclear. However, voltammograms for these complexes obtained in CH$_2$Cl$_2$–0.5 mol dm$^{-3}$ NBu$^n{}_4$PF$_6$ were almost identical to those obtained in MeCN–0.1 mol dm$^{-3}$ NBu$^n{}_4$PF$_6$ (Table 3), suggesting that the species giving rise to the observed peaks in these two solvents are the same, and probably not ligand dissociated. We therefore tentatively suggest that the electroactive species present for **3–6** are the intact [Pd(L)L$^2$]$^{n+}$ (L = 2Cl$^-$ or cat$^{2-}$, $n$ = 0; L = acac$^-$, $n$ = 1) complexes. Cyclic voltammograms of **1** and **2** were measured in MeCN only, because of the insolubility of these compounds in chlorinated solvents.

The Fe$^{II}$–Fe$^{III}$ couples for L$^1$ and L$^2$ are essentially identical, and within the usual range for ferrocenes substituted by *N*-heterocycles, including L$^3$.[8,10a–c,11] The shifts observed upon metal co-ordination of L$^2$ are similar to those observed for other ferrocenyl N-heterocyclic ligands,[11] including those such as fterpy,[10c,11] in which the ferrocene Fe atom lies > 7.5 Å from the bound metal ion. This suggests that through-space effects play little part in the electronic interactions between the pendant ferrocenyl moiety and co-ordinated metal ion in such complexes. There is a rough correlation between the electron-richness of the ferrocene ring and the Fe$^{II}$–Fe$^{III}$ half-potential, in that the orange complexes examined (**1** and **5**), which have higher-wavelength ferrocenyl d–d maxima and are more electron rich, have less-positive $E_{\frac{1}{2}}$ values than the red compounds (**2** and **6**). In particular, $E_{\frac{1}{2}}$ (Fe$^{II}$–Fe$^{III}$) for **2** is 120 mV more positive than that of **1**, as expected on inductive grounds. The exception to this trend is **3**, whose Fe$^{II}$–Fe$^{III}$ potential is essentially identical to that of **1**, despite the very different d–d maxima shown by these two complexes; the reason for this deviation is unclear.

In addition to the Fe$^{II}$–Fe$^{III}$ couple, complex **5** exhibits an equal-intensity second, quasi-reversible oxidation ($I_{pc}:I_{pa}$ = 0.4:1 at $\nu$ = 100 mV s$^{-1}$), with associated weak daughter reductions at $E_{pc}$ = −0.41 and −0.78 V. Given the similarity of this more positive $E_{\frac{1}{2}}$ value to previously reported ligand oxidation potentials for other square-planar palladium(II)–catecholate–diimine complexes,[26] we assign this second process as a cat$^{2-}$ ligand oxidation. All complexes studied also exhibit an irreversible reduction at $E_{pc}$ = −1.7 to −2.1 V with no associated daughter wave or desorption spike, which we tentatively assign to a Pd-based reductive process.

## Experimental

All manipulations were carried out in air, unless otherwise stated. Diglyme was dried over sodium before use. All other solvents, 1-acetylferrocene (Avocado), Hacac, dppe, cod, nbd (Lancaster), K$_2$[PdCl$_4$], PdCl$_2$ and PtCl$_2$ (Fluorochem) were used as supplied. The complexes [MCl$_2$(NCPh)$_2$] (M = Pd or Pt),[27] [{PdCl(C$_3$H$_5$)}$_2$],[28] [{PtCl(C$_3$H$_5$)}$_4$],[29] [PdCl$_2$(cod)][30] and [PdCl$_2$(dppe)][31] were prepared by the literature methods, while Na(acac) was precipitated from a 1 : 1 mixture of Hacac and NaOH in MeOH.

### Syntheses

**3(5)-(Ferrocen-1-yl)pyrazole L$^1$.** This was prepared according to the method of Niedenzu and co-workers.[7] (Found: C, 62.0; H, 4.80; N, 11.1. Calc. for $C_{13}H_{12}FeN_2$: C, 61.9; H, 4.78; N, 11.1%), m.p. 149–151 °C (decomp.) (lit.,[1a,7] 148–152, 148–149 °C). The $^1$H and $^{13}$C NMR and electron-impact (EI) mass spectra of L$^1$ matched those previously reported for this compound.[7,32]

**3-(Ferrocen-1-yl)-1-(pyridin-2-yl)pyrazole L$^2$.** A mixture of L$^1$ (20.0 g, 0.079 mol) and KH (3.2 g, 0.079 mol) was stirred in diglyme (100 cm$^3$) under N$_2$ for 1 h, giving a gelatinous orange precipitate. 2-Bromopyridine (12.6 g, 0.079 mol) was then added, and the mixture stirred under N$_2$ at 130 °C for 3 d. The solution was quenched with an equal volume of water, and refrigerated overnight. The resultant dark brown precipitate was filtered off, washed with water, and dried over P$_2$O$_5$. The product was extracted from this crude solid with hot hexanes, yielding an orange powder upon cooling which was recrystallised from hexanes. This product was used for the complexation studies, but contained approximately 5% unreacted L$^1$ according to $^1$H NMR spectroscopy. Yield 9.7 g, 37%. Recrystallisation from $CH_2Cl_2$–hexanes afforded orange-brown blocks, with substantial solubility losses (Found: C, 65.3; H, 4.50; N, 12.7. Calc. for $C_{18}H_{15}FeN_3$: C, 65.7; H, 4.58; N, 12.8%), m.p. 146–148 °C. EI mass spectrum: *m/z* 329 ($M^+$), 328 ($[M - H]^+$) with correct isotopic distributions. NMR spectra ($CDCl_3$, 293 K): $^1$H; δ 8.51 (d, *J* 2.6, 1 H, H$^5$ of pz), 8.39 (br d, *J* 4.9, 1 H, H$^6$ of py), 8.02 (d, *J* 8.2, 1 H, H$^3$ of py), 7.80 (ddd, *J* 8.3, 7.4 and 1.8, 1 H, H$^4$ of py), 7.13 (dd, *J* 7.4 and 4.9, 1 H, H$^5$ of py), 6.51 (d, *J* 2.6, 1 H, H$^4$ of pz), 4.78 (t, *J* 1.8, 2 H, H$^2$ + H$^5$ of ferrocenyl), 4.32 (t, *J* 1.8 Hz, 2 H, H$^3$ + H$^4$ of ferrocenyl), and 4.09 (s, 5 H, $C_5H_5$); $^{13}$C, δ 153.6, 151.6 (C$^2$ of py + C$^3$ of pz), 148.0 (C$^6$ of py), 138.6 (C$^4$ of py), 127.6 (C$^5$ of pz), 120.8, 112.4 (C$^3$ and C$^5$ of py), 106.0 (C$^4$ of pz), 77.9 (C$^1$ of ferrocenyl), 69.6 ($C_5H_5$), 68.8 (C$^2$ and C$^5$ of ferrocenyl) and 66.9 (C$^3$ and C$^4$ of ferrocenyl).

**$[Pd(C_3H_5)(L^2)]PF_6$ 1.** A mixture of L$^2$ (0.15 g, 4.56 × 10$^{-4}$ mol), $[\{PdCl(C_3H_5)\}_2]$ (0.083 g, 2.28 × 10$^{-4}$ mol) and $NH_4PF_6$ (0.074 g, 4.56 × 10$^{-4}$ mol) in $CH_2Cl_2$ (25 cm$^3$) was stirred for 1 h at room temperature, yielding an orange solution and white precipitate. The solution was filtered and evaporated until the product began to precipitate. Addition of an equal volume of diethyl ether and overnight storage at −30 °C gave orange microcrystals, which were recrystallised from MeCN–$Et_2O$. Yield 0.21 g, 73% (Found: C, 40.6; H, 3.32; N, 6.7. Calc. for $C_{21}H_{20}F_6FeN_3PPd$: C, 40.6; H, 3.24; N, 6.8%). FAB mass spectrum: *m/z* 476 $\{[^{106}PdL^2(C_3H_5)]^+\}$, 434 $([^{106}PdL^2 - H]^+)$, 329 $([L^2]^+)$ with correct isotopic distributions. NMR spectra ($CD_3CN$, 293 K): $^1$H, δ 8.59 (br d, *J* 5.0, 1 H, H$^6$ of py), 8.51 (d, *J* 2.6, 1 H, H$^5$ of pz), 8.23 (dd, *J* 8.4 and 7.7, 1 H, H$^4$ of py), 7.91 (d, *J* 8.4, 1 H, H$^3$ of py), 7.47 (dd, *J* 7.7 and 5.0, 1 H, H$^5$ of py), 7.01 (d, *J* 2.6, 1 H, H$^4$ of pz), 5.76 (tt, *J* 12.5 and 7.1, 1 H, allyl CH), 4.81 (br s, 2 H, H$^2$ + H$^5$ of ferrocenyl), 4.52 (br s, 2 H, H$^3$ + H$^4$ of ferrocenyl), 4.20 (s, 5 H, $C_5H_5$), 4.16 (d, *J* 7.1, 2 H, allyl *syn*-$CH_2$) and 3.47 (d, 12.5 Hz, 2 H, allyl *anti*-$CH_2$); $^{13}$C, δ 158.9 (C$^2$ of py), 153.1 (C$^6$ of py), 150.4 (C$^3$ of pz), 143.1 (C$^4$ of py), 131.8 (C$^5$ of pz), 124.2 (C$^3$ of py), 118.7, 113.2, 112.3 (C$^5$ of py + C$^4$ of pz + allyl CH), 75.9 (C$^1$ of ferrocenyl), 71.1, 70.3 (C$^2$–C$^5$ of ferrocenyl and $C_5H_5$) and 64.5 (allyl $CH_2$).

**$[Pt(C_3H_5)(L^2)]PF_6$ 2.** Method as for **1**, using $[\{PtCl(C_3H_5)\}_4]$ (0.12 g, 1.14 × 10$^{-4}$ mol). The product formed deep red microcrystals from MeCN–$Et_2O$. Yield 0.20 g, 63% (Found: C, 35.5; H, 2.91; N, 5.9. Calc. for $C_{21}H_{20}F_6FeN_3PPt$: C, 35.5; H, 2.84; N, 5.9%). FAB mass spectrum: *m/z* 565 $\{[^{195}PtL^2(C_3H_5)]^+\}$, 523 $([^{195}PtL^2 - H]^+)$, 444 $\{[^{195}PtL^2 - Fe(C_5H_5)]^+\}$, 329 $([L^2]^+)$ with correct isotopic distributions. NMR spectra ($CD_3CN$, 293 K): $^1$H, δ 8.88 [dd, 5.6 and *J* 0.9, *J*(Pt–H) 35, 1 H, H$^6$ of py], 8.58 [d, *J* 3.2, *J*(Pt–H) 4, 1 H, H$^5$ of pz], 8.34 (ddd, *J* 8.5, 7.6 and 1.6, 1 H, H$^4$ of py), 7.99 (d, *J* 8.5, *J*(Pt–H) 3, 1 H, H$^3$ of py], 7.48 (dd, *J* 7.6 and 5.6, 1 H, H$^5$ of py), 7.11 [d, *J* 3.2, *J*(Pt–H) 14, 1 H, H$^4$ of pz], 4.88 (br s, 1 H), 4.81 (br s, 1 H, H$^2$ + H$^5$ of ferrocenyl), 4.67 [tt, *J* 12.5 and 7.1, *J*(Pt–H) 83, 1 H, allyl CH], 4.55 (br s, 2 H, H$^3$ + H$^4$ of ferrocenyl), 4.22 (s, 5 H, $C_5H_5$), 4.15 [d, *J* 6.6, *J*(Pt–H) obscured, 1 H, allyl *syn*-$CH_2$], 3.71 [d, *J* 6.6, *J*(Pt–H) 24, 1 H, allyl *syn*-$CH_2$], 2.94 [d, *J* 11.6, *J*(Pt–H) 76, 1 H, allyl *anti*-$CH_2$], and 2.61 [d, 11.9, *J*(Pt–H) 73 Hz, 1 H, allyl *anti*-$CH_2$]; $^{13}$C, δ 158.9 (*J* 92, C$^2$ of py), 153.5 (*J* 50, C$^6$ of py), 149.7 (*J* < 10, C$^3$ of pz), 143.8 (*J* < 10, C$^4$ of py), 132.2 (*J* 19, C$^5$ of pz), 124.9 (*J* 41 C$^3$ of py), 113.3 (*J* < 10, C$^4$ of pz), 113.1 (*J* 16, C$^5$ of py), 105.6 (*J* 89, allyl CH), 75.5 (C$^1$ of ferrocenyl), 71.6, 71.4, 71.0, 70.4 (C$^2$–C$^5$ of ferrocenyl), 71.2 ($C_5H_5$), 48.7 (*J* 247, allyl $CH_2$) and 45.0 (*J* 243 Hz, allyl $CH_2$).

**$[PdCl_2(L^2)]$ 3.** Filtered solutions of L$^2$ (0.15 g, 4.56 × 10$^{-4}$ mol) and $[PdCl_2(NCPh)_2]$ (0.17 g, 4.56 × 10$^{-4}$ mol) in minimum volumes of $CH_2Cl_2$ were mixed, yielding a deep red solution. Overnight storage at −50 °C gave red needles, which were washed with hexanes and dried *in vacuo*. Yield 0.17 g, 74% (Found: C, 42.5; H, 2.85; N, 8.3. Calc. for $C_{18}H_{15}Cl_2FeN_3Pd$: C, 42.7; H, 2.98; N, 8.3%). FAB mass spectrum: *m/z* 505 $([^{106}Pd(L^2)^{35}Cl_2]^+)$, 470 $([^{106}Pd(L^2)^{35}Cl]^+)$, 435 $([^{106}PdL^2]^+)$, 329 $([L^2]^+)$ with correct isotopic distributions. NMR spectrum ($CDCl_3$, 293 K): $^1$H, δ 9.01 (d, *J* 4.8, 1 H, H$^6$ of py), 8.32 (d, *J* 2.6, 1 H, H$^5$ of pz) 8.08 (d, *J* 8.3, 1 H, H$^3$ of py), 7.65 (dd, *J* 8.3 and 7.1, 1 H, H$^4$ of py), 7.15 (dd, *J* 7.1 and 4.8, 1 H, H$^5$ of py), 6.76 (d, *J* 2.6, 1 H, H$^4$ of pz), 4.92 (t, *J* 1.8 Hz, 2 H, H$^2$ + H$^5$ of ferrocenyl), 4.39 (t, *J* 1.8, 2 H, H$^3$ + H$^4$ of ferrocenyl) and 4.06 (s, 5 H, $C_5H_5$).

**$[Pd(C_2O_4)(L^2)]$ 4.** A mixture of $K_2C_2O_4$ (0.032 g, 1.98 × 10$^{-4}$ mol) and complex **3** (0.10 g, 1.98 × 10$^{-4}$ mol) in MeOH (25 cm$^3$) was stirred for 16 h at room temperature, yielding a bright orange precipitate which was filtered off, washed copiously with MeOH and $Et_2O$, and dried *in vacuo*. Yield 0.070 g, 68% (Found: C, 44.6; H, 2.83; N, 7.9. Calc. for $C_{20}H_{15}FeN_3O_4Pd$: C, 45.9; H, 2.89; N, 8.0%). FAB mass spectrum: *m/z* 523 $\{[^{106}PdL^2(C_2O_4)]^+\}$, 434 $([^{106}PdL^2 - H]^+)$, 329 $([L^2]^+)$ with correct isotopic distributions.

**$[Pd(cat)(L^2)]$ 5.** To a solution of catechol (0.022 g, 1.98 × 10$^{-4}$ mol) in methanolic NaOH (32 cm$^3$ of a 0.5 mol dm$^{-3}$ solution) was added solid complex **3** (0.10 g, 1.98 × 10$^{-4}$ mol). The resultant suspension was stirred for 16 h at room temperature, during which time the solid became orange-brown. This precipitate was filtered off, washed with EtOH and $Et_2O$ and dried *in vacuo*. Yield 0.077 g, 72% (Found: C, 52.1; H, 3.43; N, 7.6. Calc. for $C_{24}H_{19}FeN_3O_2Pd$: C, 53.0; H, 3.52; N, 7.7%). FAB mass spectrum: *m/z* 543 $\{[^{106}PdL^2(cat)]^+\}$, 435 $([^{106}PdL^2]^+)$, 329 $([L^2]^+)$ with correct isotopic distributions.

**$[Pd(acac)(L^2)]PF_6$ 6.** A mixture of complex **3** (0.10 g, 1.98 × 10$^{-4}$ mol), Na(acac) (0.024 g, 1.98 × 10$^{-4}$ mol) and $TlPF_6$ (0.069 g, 1.98 × 10$^{-4}$ mol) was stirred in $CH_2Cl_2$ (25 cm$^3$) at room temperature for 16 h, giving a deep red solution and white precipitate. The solution was filtered and reduced to *ca.* 5 cm$^3$ in volume. Layering with $Et_2O$ initially yielded a red oil, which solidified upon standing over a period of days. Yield 0.073 g, 54% (Found: C, 40.6; H, 3.16; N, 6.4. Calc. for $C_{23}H_{22}F_6FeN_3O_2PPd$: C, 40.6; H, 3.26; N, 6.2%). FAB mass spectrum: *m/z* 534 $\{[^{106}PdL^2(acac)]^+\}$, 434 $([^{106}PdL^2 - H]^+)$, 329 $([L^2]^+)$ with correct isotopic distributions.

## Crystallography

An orange block was cleaved from a larger crystal grown by slow diffusion of hexanes into a $CH_2Cl_2$ solution of compound L$^2$, and slowly redissolved until it reached a suitable size. Experimental details of the structure determination are given in Table 4. The structure was solved by direct methods (SHELXTL PLUS),[33] and developed by full-matrix least-squares refinement on $F^2$ (SHELXL 93).[34] While all hydrogen atoms were located in the difference map during refinement, these were placed in calculated positions during the final least-squares cycles with a common isotropic thermal parameter. Attempts to derive a disorder model for the unsubstituted $C_5H_5$ ring C(2)–C(6) were unsuccessful; the slightly larger thermal parameters for these atoms compared to the rest of the molecule presumably arise from librational motion of this group in the solid.

Atomic coordinates, thermal parameters and bond lengths and angles have been deposited at the Cambridge Crystallographic Data Centre (CCDC). See instructions for Authors, *J. Chem. Soc., Dalton Trans.*, 1996, Issue 1. Any request to the CCDC for this material should quote the full literature citation and the reference number 186/207.

**Table 4** Experimental details for the single-crystal structure determination of L$^2$

| | |
|---|---|
| Formula | $C_{18}H_{15}FeN_3$ |
| $M_r$ | 329.18 |
| Crystal habit | Orange block |
| Crystal size/mm | 0.30 × 0.25 × 0.20 |
| Crystal class | Orthorhombic |
| Space group | $P2_12_12_1$ |
| $a$/Å | 11.004(4) |
| $b$/Å | 13.919(3) |
| $c$/Å | 9.447(2) |
| $U$/Å$^3$ | 1447.0(7) |
| $Z$ | 4 |
| $D_c$/Mg m$^{-3}$ | 1.511 |
| No. data for lattice parameters | 25 |
| θ Range/° for lattice parameters | 30.0–40.0 |
| μ/mm$^{-1}$ | 1.041 |
| $F$(000) | 680 |
| $T$/K | 293(2) |
| Diffractometer | Rigaku AFC 7-R |
| Radiation (λ/Å) | Graphite-monochromated Mo-Kα (0.710 69) |
| Scan type | ω–2θ |
| Absorption correction | Empirical (ψ scans) |
| Minimum, maximum transmission | 0.933, 0.998 |
| Measured reflections | 4056 |
| Independent reflections | 3313 |
| $R_{int}$ | 0.0311 |
| Observed reflections [$I > 2\sigma(I)$] | 2911 |
| 2θ Range/° | 5–55 |
| Standards | 3 every 200 reflections |
| Variation during data collection | 0.5% decay |
| *hkl* Ranges | −14 to 14, −18 to 18, −12 to 12 |
| No. parameters | 200 |
| No. restraints | 0 |
| $R(F)$ | 0.0368 |
| $wR(F^2)$ | 0.1059 |
| Goodness of fit | 0.865 |
| Weighting scheme, $w$ | $1/[\sigma^2(F_o^2) + (0.0734P)^2 + 0.4325P]$ |
| Maximum shift/e.s.d. | 0.002 |
| $\Delta\rho_{min}, \Delta\rho_{max}$/e Å$^{-3}$ | −0.40, 0.42 |
| Flack parameter | 0.02(3) |

$R = \Sigma[|F_o| - |F_c|]/\Sigma|F_o|$, $wR = [\Sigma w(F_o^2 - F_c^2)/\Sigma wF_o^4]^{\frac{1}{2}}$, $w = 1/[\sigma^2(F_o^2) + (xP)^2 + yP]$, $P = (F_o^2 + 2F_c^2)/3$.

### Other measurements

Infrared spectra were obtained as Nujol mulls pressed between KBr windows between 400 and 4000 cm$^{-1}$ using a Perkin-Elmer Paragon 1000 spectrophotometer and UV/VIS spectra with a Perkin-Elmer Lambda 12 spectrophotometer operating between 200 and 1100 nm, in 1 cm quartz cells. Room-temperature NMR spectra were run on a Bruker DPX250 spectrometer, operating at 250.1 ($^1$H) and 62.9 MHz ($^{13}$C); low-temperature $^1$H spectra were obtained using a Bruker AM400 instrument operating at 400.1 MHz. Electron impact (EI) and positive-ion fast atom bombardment (FAB, 3-nitrobenzyl alcohol matrix) mass spectra were recorded on a Kratos MS50 spectrometer. The microanalyses (C,H,N) were performed by the University of Cambridge Department of Chemistry microanalytical service. Melting points are uncorrected. All electrochemical measurements were carried out using an Autolab PGSTAT20 voltammetric analyser, in MeCN or $CH_2Cl_2$ containing 0.1 and 0.5 mol dm$^{-3}$ $NBu^n_4PF_6$ (prepared from $NBu^n_4OH$ and $HPF_6$), respectively, as supporting electrolyte. Cyclic voltammetric experiments involved the use of a double platinum working/counter electrode and a silver-wire reference electrode; all potentials quoted in the text are referenced to an internal ferrocene–ferrocenium standard and were obtained at a scan rate of 100 mV s$^{-1}$. Molecular models, which were not energy minimised, were prepared using CHEM 3D[35] and employed the crystal structure atomic coordinates for L$^2$ [with C(18) and N(22) in exchanged sites] and literature values for Pd–N, Pd–O and intrachelate ligand distances and angles.[36]

## Acknowledgements

We thank the Royal Society (London) for a University Research Fellowship (to M. A. H.), the Commonwealth Overseas Trust and O.R.S. fund for a studentship (to N. L. C.), the EPSRC for purchase of a diffractometer, the University of Cambridge and St. Catharine's College for support.

## References

1 (*a*) K. Schlögl and A. Mohar, *Monatsh. Chem.*, 1962, **93**, 861; (*b*) K. Schlögl and H. Egger, 1963, **94**, 1054.

2 N. J. Long, *Angew. Chem., Int. Ed. Engl.*, 1995, **34**, 21.

3 M. D. Ward, *Chem. Soc. Rev.*, 1995, **24**, 121.

4 M. Sawamura and Y. Ito, *Chem. Rev.*, 1992, **92**, 857; H. B. Kagan, P. Diter, A. Gref, D. Guillaneux, A. Masson-Szymczak, F. Rebière, O. Riant, O. Samuel and S. Taudien, *Pure Appl. Chem.*, 1996, **68**, 29.

5 S. Trofimenko, *Prog. Inorg. Chem.*, 1986, **34**, 115; P. K. Byers, A. J. Canty and R. T. Honeyman, *Adv. Organomet. Chem.*, 1992, **34**, 1; S. Trofimenko, *Chem. Rev.*, 1993, **93**, 943; N. Kitajima and W. B. Tolman, *Prog. Inorg. Chem.*, 1995, **43**, 419; G. Parkin, *Adv. Inorg. Chem.*, 1995, **42**, 291.

6 E. C. Constable and P. J. Steel, *Coord. Chem. Rev.*, 1989, **93**, 205.

7 K. Niedenzu, J. Serwatowski and S. Trofimenko, *Inorg. Chem.*, 1991, **30**, 524.

8 N. Chabert, L. Jacquet, C. Marzin and G. Tarrago, *New J. Chem.*, 1995, **19**, 443.

9 (*a*) P. D. Beer, O. Kocian and R. J. Mortimer, *J. Chem. Soc., Dalton Trans.*, 1990, 3283; (*b*) I. R. Butler and J.-L. Roustan, *Can. J. Chem.*, 1990, **68**, 2212; (*c*) I. R. Butler, *Organometallics*, 1992, **11**, 74; (*d*) I. R. Butler, N. Bourke, L. J. Hobson and H. Findenegg, *Polyhedron*, 1992, **11**, 2435; (*e*) I. R. Butler, *Polyhedron*, 1992, **11**, 3117; (*f*) A. C. Benniston, V. Goulle, A. Harriman, J.-M. Lehn and B. Marczinke, *J. Phys. Chem.*, 1994, **98**, 7798; (*g*) I. R. Butler, M. Kalaji, L. Nehrlich, M. Hursthouse, A. I. Karaulov and K. M. Abdul Malik, *J. Chem. Soc., Chem. Commun.*, 1995, 459.

10 (*a*) J.-C. Chambron, C. Coudret and J.-P. Sauvage, *New J. Chem.*, 1992, **16**, 361; (*b*) B. Farlow, T. A. Nile, J. L. Walsh and A. T. McPhail, *Polyhedron*, 1993, **12**, 2891; (*c*) E. C. Constable, A. J. Edwards, R. Martínez-Máñez, P. R. Raithby and A. M. W. Cargill Thompson, *J. Chem. Soc., Dalton Trans.*, 1994, 645; (*d*) I. R. Butler, S. J. McDonald, M. B. Hursthouse and K. M. Abdul Malik, *Polyhedron*, 1995, **14**, 529.

11 E. C. Constable, R. Martínez-Máñez, J. V. Walker and A. M. W. Cargill Thompson, *J. Chem. Soc., Dalton Trans.*, 1994, 1585; E. C. Constable, A. J. Edwards, R. Martínez-Máñez and P. R. Raithby, *J. Chem. Soc., Dalton Trans.*, 1995, 3253.

12 M. A. Halcrow and J. E. Davies, unpublished work.

13 D. L. Jameson, J. K. Blaho, K. T. Kruger and K. A. Goldsby, *Inorg. Chem.*, 1989, **28**, 4312; D. L. Jameson and K. A. Goldsby, *J. Org. Chem.*, 1990, **55**, 4992; D. L. Christenson, C. J. Tokar and W. B. Tolman, *Organometallics*, 1995, **14**, 2148; A. T. Baker, D. C. Craig, G. Dong and A. D. Rae, *Aust. J. Chem.*, 1995, **48**, 1071.

14 J. Elguero and R. Jacquier, *J. Chim. Phys.*, 1966, 1242.

15 M. Bruix, J. de Mendoza and J. Elguero, *Tetrahedron*, 1987, **43**, 4663.

16 A. L. Llamas-Saiz, C. Foces-Foces and J. Elguero, *J. Mol. Struct.*, 1994, **319**, 231.

17 Y. Nagakawara, K. Kikukawa, M. Tagaki and T. Matsuda, *Bull. Chem. Soc. Jpn.*, 1977, **50**, 2748; J. Elguero, A. Fruchier, A. de la Hoz, F. A. Jalón, B. R. Manzano, A. Otero and F. Gómez-de la Torre, *Chem. Ber.*, 1996, **129**, 589.

18 A. Kasahara, T. Izumi and M. Maemura, *Bull. Chem. Soc. Jpn.*, 1977, **50**, 1878.

19 K. Nakamoto, *Infra-red and Raman Spectra of Inorganic and Coordination Compounds*, 4th edn., Wiley, New York, 1986.

20 (*a*) Y. S. Sohn, D. N. Hendrickson and H. B. Gray, *J. Am. Chem. Soc.*, 1971, **93**, 3603; (*b*) D. R. Kanis, M. A. Ratner and T. J. Marks, *J. Am. Chem. Soc.*, 1992, **114**, 10338.

21 J. Elguero, R. Jacquier and H. C. N. T. Duc, *Bull. Soc. Chim. Fr.*, 1966, 3744.

22 S. Toma, A. Gáplovsky, M. Hudecek and Z. Langfelderová, *Monatsh. Chem.*, 1985, **116**, 357.

23 M. Kahn and J. B. Polya, *J. Chem. Soc. C*, 1970, 85.

24 F. R. Hartley, *J. Organomet. Chem.*, 1970, **21**, 227.

25 N. Saha, D. Bhattacharyya and S. K. Kar, *Inorg. Chim. Acta*, 1982, **67**, L37.

26 A. L. Balch, *J. Am. Chem. Soc.*, 1973, **95**, 2723; S. S. Kamath, V. Uma and T. S. Srivastava, *Inorg. Chim. Acta*, 1989, **166**, 91.

27 G. K. Anderson and M. Lin, *Inorg. Synth.*, 1990, **28**, 60.

28 Y. Tatsuno, T. Yoshida and S. Otsuka, *Inorg. Synth.*, 1990, **28**, 342.

29 J. H. Lukas, *Inorg. Synth.*, 1974, **15**, 75.

30 D. Drew and J. R. Doyle, *Inorg. Synth.*, 1990, **28**, 346.

31 D. W. Meek, P. E. Nipcon and V. I. Meek, *J. Am. Chem. Soc.*, 1970, **92**, 5351.

32 C. Lopez, R. M. Claramunt, S. Trofimenko and J. Elguero, *Can. J. Chem.*, 1993, **71**, 678.

33 G. M. Sheldrick, SHELXTL PLUS, PC version, Siemens Analytical X-Ray Instruments Inc., Madison, WI, 1990.

34 G. M. Sheldrick, SHELXL 93, University of Göttingen, 1993.

35 *CHEM 3D Pro* 3.1.3, Cambridge Soft Corporation, Cambridge, MA, 1995.

36 G. B. Caygill and P. J. Steel, *J. Organomet. Chem.*, 1987, **327**, 115; G. A. Fox and C. G. Pierpont, *Inorg. Chem.*, 1992, **31**, 3718.

*Received* 14*th June* 1996; *Paper* 6/04201E